



Published in final edited form as:

*Cancer Res.* 2012 July 15; 72(14): 3492–3498. doi:10.1158/0008-5472.CAN-11-4037.

## Ultrasensitive measurement of hotspot mutations in tumor DNA in blood using error-suppressed multiplexed deep sequencing

Azeet Narayan<sup>1,\*</sup>, Nicholas J. Carriero<sup>2,\*</sup>, Scott N. Gettinger<sup>3</sup>, Jeannie Kluytenaar<sup>1</sup>, Kevin R. Kozak<sup>4</sup>, Torunn I. Yock<sup>5</sup>, Nicole E. Muscato<sup>6</sup>, Pedro Ugarelli<sup>7</sup>, Roy H. Decker<sup>1</sup>, and Abhijit A. Patel<sup>1</sup>

<sup>1</sup>Departments of Therapeutic Radiology, Yale University, New Haven, CT 06520

<sup>2</sup>Departments of Computer Science and Yale University, New Haven, CT 06520

<sup>3</sup>Departments of Internal Medicine, Yale University, New Haven, CT 06520

<sup>4</sup>Department of Human Oncology, University of Wisconsin, Madison, WI 53792

<sup>5</sup>Department of Radiation Oncology, Massachusetts General Hospital, Boston, MA 02114

<sup>6</sup>Departments of Pathology and Lawrence & Memorial Hospital, New London, CT 06320

<sup>7</sup>Departments of Hematology, Lawrence & Memorial Hospital, New London, CT 06320

### Abstract

Detection of cell-free tumor DNA in the blood has offered promise as a cancer biomarker, but practical clinical implementations have been impeded by the lack of a sensitive and accurate method for quantitation that is also simple, inexpensive, and readily scalable. Here we present an approach that uses next-generation sequencing to quantify the small fraction of DNA molecules that contain tumor-specific mutations within a background of normal DNA in plasma. Using layers of sequence redundancy designed to distinguish true mutations from sequencer misreads and PCR misincorporations, we achieved a detection sensitivity of approximately 1 variant in 5,000 molecules. In addition, the attachment of modular barcode tags to the DNA fragments to be sequenced facilitated the simultaneous analysis of more than a hundred patient samples. As proof of principle, we demonstrated the successful use of this method to follow treatment-associated changes in circulating tumor DNA levels in patients with non-small cell lung cancer. Our findings suggest that the deep sequencing approach described here may be applied to the development of a practical diagnostic test that measures tumor-derived DNA levels in blood.

### INTRODUCTION

The release of cell-free DNA into the bloodstream from dying tumor cells has been well-documented in patients with various types of cancer(1–4). There has been growing interest in trying to utilize such circulating tumor DNA (ctDNA) as a non-invasive biomarker to detect the presence of malignancy, follow treatment response, gauge prognosis, or monitor for recurrence(5, 6). Because unique somatic mutations can be used as telltale marks to distinguish tumor-derived DNA in plasma, a new class of highly specific DNA-based cancer

**Corresponding Author:** Abhijit A. Patel, Department of Therapeutic Radiology, Yale University School of Medicine, P.O. Box 208040, New Haven, CT 06520. Phone: 203-785-2971; Fax: 203-785-7482; abhijit.patel@yale.edu.

\*These authors contributed equally to this work.

**Disclosure:** The authors declare no potential conflicts of interest.

biomarkers can be envisioned with clinical applications that may complement those of conventional serum protein markers.

To more formally explore the clinical utility of ctDNA, it would be imperative to be able to sensitively and accurately measure its levels in blood. However, because mutation-harboring ctDNA can be obscured by a relative excess of background wild-type DNA, quantitation has proven to be challenging. Several innovative approaches have been developed to detect the presence or absence of low-level mutant DNA in clinical samples(7–12), but few methods are able to sensitively quantify ctDNA(13, 14).

The recent advent of next-generation, high-throughput DNA sequencing technologies presents an attractive and seemingly obvious solution to this problem. By oversampling multiple DNA molecules from a particular genomic region using an approach known as ultra-deep sequencing, it is possible to identify and enumerate rare sequence variants. But the sensitivity of this method is limited by the inherent error rate of the sequencer, since incorrectly read bases might be mistaken for true mutant copies. Indeed, mutant ctDNA has been previously reported to comprise an average of 0.2% of total plasma DNA(14) – a range in which sequencer misreads can be problematic.

Here we describe a modified deep sequencing method that demands redundancy within each clonal sequence to produce extremely high quality base-calls in short, mutation-prone regions of plasma DNA. Amplification of both mutated and wild-type sequences is carried out by unbiased PCR in a single tube, ensuring highly accurate and reproducible quantitation. The scheme is designed to have the flexibility to simultaneously analyze mutations in several genes from multiple patient samples, making it practically feasible to screen plasma samples for mutant ctDNA without prior knowledge of the tumor’s mutation profile.

## MATERIALS AND METHODS

### Patient plasma and tumor samples

Under the approval of the Human Investigation Committees at the Yale School of Medicine and at Lawrence & Memorial Hospital, 30 patients with stage I-IV NSCLC were enrolled in this study between July 2009 and July 2010. Informed consent was obtained from all patients. Most patients were recruited in the radiation oncology clinic, and underwent treatment with radiation therapy, chemotherapy, targeted systemic therapy, and/or surgery. Whenever possible, blood samples were collected from patients before starting the current course of treatment and then at subsequent times during and after treatment. A total of 117 samples were obtained. Formalin-fixed, paraffin-embedded tumor specimens were obtained for all patients with non-squamous histology whose tumors had not already been tested for mutations by a clinical laboratory, and for whom sufficient tissue was available in the block after standard pathology evaluation.

### Extraction and amplification of plasma DNA

Blood was collected in EDTA-containing tubes (Becton Dickinson) and was centrifuged at 1000 g for 10 minutes within 3 hours of collection. Plasma was transferred to cryovials, being careful to avoid the buffy coat, and was stored at –80°C until further processing. DNA was extracted from 0.2 mL of each plasma sample using the QIAamp DNA Blood Mini kit (Qiagen), according to the manufacturer’s protocol. Amplification of mutation hotspot regions was carried out in triplicate for each sample using two successive rounds of PCR, with primers designed to flank codons 12 and 13 of *KRAS*, codon 858 of *EGFR*, and codon 600 of *BRAF*. In the first round of PCR, all hotspot regions from a given sample were amplified in a multiplexed fashion. The products of these reactions were diluted 5000-fold

and then used as templates for a second round of PCR in which each hotspot was amplified separately using nested primers with sample-specific barcodes. The barcode sequences were 6 nucleotides in length, and were designed to differ from all other barcodes in the set at a minimum of 2 positions so that a single sequencing error would not lead to misclassification of samples. All PCR steps were carried out using a high-fidelity polymerase (HiFi Hotstart, Kapa Biosystems). Real-time quantitative PCR was used to determine the total concentration of mutant and wild-type DNA fragments. Details of PCR and of modular barcode attachment to gene-specific primers are included in Supplementary Materials and Methods.

### Analysis of cell line DNA

Genomic DNA was purified from human cancer cell lines using the same method used for purifying plasma DNA, after suspending cells in 0.2 mL of phosphate-buffered saline. The following cell lines were used: A549 (having a KRAS Gly12Ser mutation; gift of J. Weidhaas, Yale), H1957 (having an EGFR Leu858Arg mutation; gift of J. Weidhaas, Yale), and YUSAC (having a BRAF Val600Glu mutation; gift of R. Halaban, Yale). Cells were passed in culture for no more than 6 months after being thawed from original stocks. Because cell lines were used only for analysis of short regions of genomic DNA, authentication of lines by our laboratory was limited to sequencing of those regions. To test the performance of the deep sequencing method for a particular gene, DNA derived from cells known to be either mutant or wild-type with respect to that gene was mixed in various ratios between 10,000:1 and 1:10,000. Cell line DNA samples were then amplified and sequenced according to the same methods that were used for plasma DNA.

### Ultra-deep sequencing

Barcoded PCR products from all samples were mixed to create 3 separate pools, each corresponding to one set of replicate reactions. IlluminaTruSeq sequencing adapters with different indices were ligated to each of the three amplicon pools and were gel-purified as recommended by the manufacturer. All samples were loaded onto a single lane of an Illumina HiSeq2000 flow cell, and were subjected to paired-end sequencing (75 base pairs per read). Sequencing details and modifications to standard Illumina protocols are described in Supplementary Materials and Methods.

### Data analysis

All sequences were initially sorted into 3 replicate groups based on the adapter index sequence using Illumina's de-multiplexing algorithm. A computer script was written to filter, assort, align, and count millions of paired-end sequences within each group. First, a read-pair was assigned to a sample-specific data bin based on the barcode of each read in the pair. Then, based on PCR primer sequences, the pair was assigned to one of the reference genes. Next, the longest stretch of perfect sequence agreement between each pair of reads was determined, and this was used to align the reads to the reference sequence for the gene. A read pair was discarded if either member did not pass Illumina filtering or a nucleotide was reported to be "."; if there was an inconsistency in barcodes, strands, or PCR tags; or if their region of perfect sequence agreement was less than 36 nucleotides in length. Finally, variant sequences confirmed by reads from both strands were identified and counted within each data bin based on comparison to the reference sequence. The mean counts of variant sequences corresponding to known hotspot mutations were calculated from the 3 replicate data bins for each sample. The number of copies of mutant DNA fragments in a plasma sample was determined by using real-time PCR to measure the total concentration of both mutant and wild-type DNA fragments, and then multiplying this value by the fraction of mutant molecules determined by deep sequencing. A mutation was considered to be undetectable if the number of mutant copies in the plasma sample was calculated to be less

than one. Further details are available in Supplementary Materials and Methods. The full computer code, which we call OPAL for “Overlapped Paired-end ALignment”, is available upon request.

### Confirmation of mutations in tumor tissue

Genomic DNA was isolated from paraffin-embedded tumor tissue samples using the QuickExtract FFPE DNA Extraction Kit (Epicentre). Mutation hotspot regions of *KRAS*, *BRAF*, and *EGFR* were amplified using the same PCR primers that were used in the first round of PCR described above. Sanger sequencing was performed on gel-purified amplicons, and mutations were identified from chromatograms using Mutation Surveyor software (Softgenetics).

## RESULTS

### Error suppression reveals low-abundance variants

To determine the relative abundance of tumor-specific mutations, we performed massively parallel sequencing of PCR amplicons derived from plasma DNA fragments containing known mutation hotspots. Thousands of clonal sequence reads from each plasma sample were compared to reference sequences in order to identify and quantify variants. For proof of concept, we restricted the analysis to frequently mutated codons within 3 oncogenes that commonly develop somatic mutations in various malignancies: codons 12 and 13 of *KRAS*, codon 600 of *BRAF*, and codon 858 of *EGFR*. By designing PCR primers that flank very short regions (<50 bp) surrounding these mutation hotspots, we could ensure adequate amplification of highly fragmented plasma DNA and achieve greater sequence depth. Modular attachment of DNA barcode tags to the 5'-ends of the PCR primers allowed sequencing of up to 256 DNA samples in batch (Fig. 1A and Supplementary Fig. S1). We obtained a median depth of 108,467 read pairs per mutation site per sample after filtering and de-multiplexing a total of 86,359,980 raw sequences generated on a single lane of an Illumina HiSeq 2000 flow cell.

Importantly, the design of short PCR amplicons enabled us to devise a sequencing strategy that could distinguish mutant from wild-type DNA molecules with very high confidence. We modified Illumina's paired-end sequencing mode to achieve partial overlap of 75 base-pair bidirectional reads obtained sequentially from the forward and reverse strands of each clonal DNA cluster on the flow cell (Fig. 1B). Mutation hotspots were included in the overlapping sequence region so that the hotspot within each clone would be read from one strand and then proofread from the opposite strand. By discarding clones that did not have perfect sequence agreement between the two paired-end reads, we were able to eliminate the vast majority of sequencer-generated errors. Imperfect sequence agreement was found in 22% of read pairs that had already passed Illumina's chastity filter. Similar to prior reports(15, 16), we observed a median error frequency of 0.31% per base when directly comparing single reads derived from either strand of wild-type control samples to known reference sequences. The frequency of such errors was reduced to 0.07% per base in the region of overlap after removing read pairs that lacked sequence consistency.

Any remaining errors were highly unlikely to be caused by coincidentally consistent misreads from opposite ends of a clone. Rather, most of these errors were probably present within the DNA molecules being sequenced, introduced by polymerase misincorporations or DNA damage. To further discriminate true mutations from such errors, we carried out all amplification and processing steps in triplicate and determined the mean of the three mutation counts. This was done based on the premise that true mutations would be reproducibly counted in all three instances, whereas counts from randomly occurring errors

would be more variable (recognizing that the distribution of errors is not entirely random). Using this approach, we were able to reduce the frequency of miscalls of specific mutations from known wild-type samples to a median value of 0.014% (interquartile range [IQR]: 0.0052% to 0.023%; Wild-type DNA was obtained from A549 cells for testing BRAF and EGFR mutations and from YUSAC cells for testing KRAS mutations; Supplementary Table S1). Suppression of errors in this manner permitted rare mutations to be identified with a high degree of certainty (Fig. 2).

### Sensitive and accurate quantitation of mutant DNA

Next, we tested the ability of this deep sequencing approach to measure mutant and wild-type DNA levels over a broad range of relative concentrations. Genomic DNA from *KRAS*-, *BRAF*-, or *EGFR*-mutant cancer cell lines was mixed in different ratios, and then subjected to amplification and deep sequencing. We found that mutant DNA could be accurately and reproducibly measured in a linear manner over approximately 7 to 8 orders of magnitude and down to levels of approximately 1 in 5,000 molecules (Fig. 3). Also, by testing combinations of DNA from multiple mutant cell lines, we confirmed the ability of the assay to simultaneously quantify more than one mutation from a given sample.

### Monitoring ctDNA levels in cancer patients

To validate this method with clinical samples, we analyzed plasma collected from patients with non-small cell lung cancer (NSCLC) at various times before, during, or after treatment. Patients were enrolled in the study (and their plasma DNA was tested) without prior knowledge of the mutation status of their tumors. A total of 117 samples were obtained from 30 patients (17 patients with adenocarcinoma, 9 with undifferentiated NSCLC, and 4 with squamous cell carcinoma). *KRAS* Gly12Asp, Gly12Val, Gly12Cys, or Gly13Asp point-mutations were detectable in the plasma DNA of 6 patients out of 26 with adenocarcinoma or undifferentiated NSCLC. As expected, no *KRAS* mutations were found in specimens from patients with squamous cell carcinoma. *BRAF* and *EGFR* mutations were not detectable in any plasma samples. This was somewhat surprising for *EGFR*, which has a reported prevalence of activating mutations in NSCLC of approximately 10% (17–19). However, evaluation of 21 available tumor tissue specimens confirmed the absence of *EGFR* mutations in this population (mutations occurring outside of the sequenced hotspot region may have been missed). We found the presence or absence of *KRAS* mutations in all tested tumor samples to be concordant with the findings in plasma: 5 patients had identical *KRAS* mutations in both tumor and plasma, and 16 patients had no *KRAS* mutations detected from either source. Tumor tissue was unavailable or insufficient for 1 patient with mutant *KRAS* in the plasma, and for 4 patients with no plasma mutations. Supplementary Table S2 lists the clinical characteristics and mutation findings for all patients in the study.

For patients with detectable plasma DNA mutations, we were able to follow changes in measured ctDNA levels in the context of therapeutic interventions or disease progression. To determine the absolute concentration of mutant *KRAS* DNA fragments in a plasma sample, we measured the total concentration of *KRAS* fragments by real-time PCR, and then multiplied this value by the fraction of mutant molecules determined by deep sequencing. The median concentration among samples with detectable mutations was 5,694 mutant *KRAS* molecules per mL (IQR: 2,655 to 25,123). Time-courses of mutant ctDNA measurements for patients who had 3 or more samples collected are shown in Fig. 4 (data for patients with fewer measurements are shown in Supplementary Fig. S2). In two cases, we observed a decrease in the ctDNA level upon treatment with radiation and/or systemic therapy. Aggressive progression of metastatic disease in a different patient was accompanied by a substantial rise in ctDNA. In another two cases, we saw an increase in ctDNA levels



shortly after initiating treatment, perhaps because more tumor DNA was released into the bloodstream as cancer cells were being killed.

## DISCUSSION

The deep sequencing approach described above demonstrates the successful application of principles that we believe could form the basis of a practical diagnostic test to measure tumor-derived DNA levels in blood. The accuracy and sensitivity provided by the error suppression strategy enables quantitation of mutant ctDNA within a clinically informative range of concentrations. The multiplexing scheme allows parallel analysis of mutations within several genes from hundreds of patient samples with low marginal cost and effort. Thus, analysis need not be limited to mutations that are already identified in a patient's tumor tissue. Moreover, the flexibility and scalability afforded by the modular barcoding approach makes it fairly easy to customize the panel of genes to be evaluated according to the prevalence of mutations in different malignancies. These features suggest a potential application of this technology that takes advantage of the cancer specificity of mutant ctDNA: early cancer detection. In order to be practically useful for cancer screening, however, such an assay would have to include analysis of mutations in a larger panel of genes to maximize the probability of detecting ctDNA. Also, extensive testing of healthy volunteers would be required to determine the false-positive rate and positive predictive value of the assay before proceeding with clinical screening studies. While much work remains to be done, the methods presented in this paper illustrate how next-generation sequencing can bring us a step closer to evaluation of ctDNA as a non-invasive biomarker for cancer screening.

Although many other techniques have been developed to analyze ctDNA, we believe that this deep sequencing approach offers important advantages. Several commonly used strategies facilitate detection of rare mutant DNA molecules from clinical specimens by preferentially amplifying mutant relative to wild-type sequences(7–12). While these methods have excellent sensitivity, they are unable to provide quantitative information due to the poor reproducibility of biased amplification. The most sensitive existing methods for quantifying ctDNA(13, 20) require custom primers or probes to be synthesized for a specific known mutation in a patient's tumor, making it impractical to use these assays for cancer screening. Kinde et al. recently described an elegant and powerful error-reduction strategy that enables highly sensitive quantitation of DNA variants using massively parallel sequencing(21). However, this approach was not designed to analyze multiple amplicons from samples containing limited DNA, and was not tested on clinical specimens.

A notable limitation of our method is the need to focus on short, mutation-prone regions of DNA because of length constraints in the overlapping portion of paired-end reads. This may preclude evaluation of inactivating mutations that can occur at numerous possible locations within tumor suppressor genes. Nonetheless, many tumor suppressor genes would be amenable to analysis by this method because their mutations tend to be clustered within short domains (such as the region of *TP53* that encodes the DNA binding domain). Also, as sequencing technologies improve, read lengths are likely to become less constraining. Another limitation of our study was the small number of patients whose mutant ctDNA we were able to measure. Had we selectively enrolled patients with known tumor mutations, we would have likely seen more cases with measurable ctDNA. However, we chose to test the performance of the method on an unselected population of patients with NSCLC, and did observe congruence between mutations from plasma and tumor tissue in this small sample set. By including a larger panel of cancer-specific mutations in future studies, we expect to be able to measure mutant ctDNA in a higher percentage of patients. Finally, although we report a limit of detection of approximately 1 variant in 5,000 molecules, one must keep in

mind that mutant counts would need to be several-fold above background in order to guide clinical decisions.

Practical considerations such as cost and turnaround time must also be factored into any analysis of the potential utility of a new technology. Although the capital equipment costs of next-generation sequencing are presently very high, they are predicted to drop substantially as the technologies mature. Because barcoding allows multiple samples to be analyzed in a single sequencing run, the current cost per sample is well under 100 U.S. dollars. When we performed the described experiments, a 75 base-pair, paired-end run with indexing took approximately 9 to 10 days of sequencer time. If 3 to 4 days are added for sample preparation and computational analysis, the resultant turnaround time might be considered to be impractical for a clinical test. But sequencer speeds have improved dramatically in just the past several months and this trend is likely to continue. Thus, it does not appear that cost and time will remain significant impediments for much longer.

Error-suppressed deep sequencing may find applications in other scenarios where quantitation of low-abundance DNA variants would be informative. The diagnostic utility of rare cancer-associated mutations is being investigated in biological specimens such as lymph nodes, stool, pleural fluid, peritoneal fluid, and urine. Outside of oncology, analysis of nucleic acid variants has been useful in HIV medicine(22), organ transplantation(23), and prenatal diagnosis(24). Additional unanticipated uses may become apparent as next-generation sequencing technologies continue to be repurposed beyond their originally intended applications.

## Supplementary Material

Refer to Web version on PubMed Central for supplementary material.

## Acknowledgments

We thank A. McKeon for help with Human Investigation Committee documentation; J. Lubner and M. Mahajan for assistance with next-generation sequencing; J. Weidhaas and R. Halaban for providing cell lines; L. Harrington, H. Schilke, T. Chapman, E. Washington, and N. Lacks for assistance with phlebotomy; and P. Glazer and D. Brash for valuable comments on the manuscript.

**Financial Support:** This work was supported by the Yale Cancer Center, the American Cancer Society, the Kalimeris Fund, a Rudolph Anderson Fellowship, a Leslie Warner fellowship, and CTSA grant numbers UL1RR024139 and 5KL2RR024138 from the National Center for Research Resources, a component of the US National Institutes of Health.

## REFERENCES

1. Vasioukhin V, Anker P, Maurice P, Lyautey J, Lederrey C, Stroun M. Point mutations of the N-ras gene in the blood plasma DNA of patients with myelodysplastic syndrome or acute myelogenous leukaemia. *Br J Haematol.* 1994; 86:774–779. [PubMed: 7918071]
2. Kimura T, Holland WS, Kawaguchi T, et al. Mutant DNA in plasma of lung cancer patients: potential for monitoring response to therapy. *Ann N Y Acad Sci.* 2004; 1022:55–60. [PubMed: 15251940]
3. Diehl F, Li M, Dressman D, et al. Detection and quantification of mutations in the plasma of patients with colorectal tumors. *Proc Natl Acad Sci USA.* 2005; 102:16368–16373. [PubMed: 16258065]
4. Schwarzenbach H, Chun FK, Lange I, et al. Detection of tumor-specific DNA in blood and bone marrow plasma from patients with prostate cancer. *Int J Cancer.* 2007; 120:1465–1471. [PubMed: 17205532]

5. Gahan PB, Swaminathan R. Circulating nucleic acids in plasma and serum. Recent developments. *Ann N Y Acad Sci.* 2008; 1137:1–6. [PubMed: 18837917]
6. Kaiser J. Medicine. Keeping tabs on tumor DNA. *Science.* 2010; 327:1074. [PubMed: 20185705]
7. Li J, Wang L, Mamon H, Kulke MH, Berbeco R, Makrigiorgos GM. Replacing PCR with COLD-PCR enriches variant DNA sequences and redefines the sensitivity of genetic testing. *Nat Med.* 2008; 14:579–584. [PubMed: 18408729]
8. Kopreski MS, Benko FA, Kwee C, et al. Detection of mutant K-ras DNA in plasma or serum of patients with colorectal cancer. *Br J Cancer.* 1997; 76:1293–1299. [PubMed: 9374374]
9. Sun X, Hung K, Wu L, Sidransky D, Guo B. Detection of tumor mutations in the presence of excess amounts of normal DNA. *Nat Biotechnol.* 2002; 20:186–189. [PubMed: 11821866]
10. Li J, Berbeco R, Distel RJ, Janne PA, Wang L, Makrigiorgos GM. s-RT-MELT for rapid mutation scanning using enzymatic selection and real time DNA-melting: new potential for multiplex genetic analysis. *Nucleic Acids Res.* 2007; 35:e84. [PubMed: 17545195]
11. Lehman TA, Scott F, Seddon M, et al. Detection of K-ras oncogene mutations by polymerase chain reaction-based ligase chain reaction. *Anal Biochem.* 1996; 239:153–159. [PubMed: 8811898]
12. Jacobson DR, Mills NE. A highly sensitive assay for mutant ras genes and its application to the study of presentation and relapse genotypes in acute leukemia. *Oncogene.* 1994; 9:553–563. [PubMed: 8290266]
13. Shi C, Eshleman SH, Jones D, et al. LigAmp for sensitive detection of single-nucleotide differences. *Nat Methods.* 2004; 1:141–147. [PubMed: 15782177]
14. Diehl F, Schmidt K, Choti MA, et al. Circulating mutant DNA to assess tumor dynamics. *Nat Med.* 2008; 14:985–990. [PubMed: 18670422]
15. Quail MA, Kozarewa I, Smith F, et al. A large genome center's improvements to the Illumina sequencing system. *Nat Methods.* 2008; 5:1005–1010. [PubMed: 19034268]
16. Nazarian R, Shi H, Wang Q, et al. Melanomas acquire resistance to B-RAF(V600E) inhibition by RTK or N-RAS upregulation. *Nature.* 2010; 468:973–977. [PubMed: 21107323]
17. Paez JG, Janne PA, Lee JC, et al. EGFR mutations in lung cancer: correlation with clinical response to gefitinib therapy. *Science.* 2004; 304:1497–1500. [PubMed: 15118125]
18. Lynch TJ, Bell DW, Sordella R, et al. Activating mutations in the epidermal growth factor receptor underlying responsiveness of non-small-cell lung cancer to gefitinib. *N Engl J Med.* 2004; 350:2129–2139. [PubMed: 15118073]
19. Pao W, Miller V, Zakowski M, et al. EGF receptor gene mutations are common in lung cancers from "never smokers" and are associated with sensitivity of tumors to gefitinib and erlotinib. *Proc Natl Acad Sci U S A.* 2004; 101:13306–13311. [PubMed: 15329413]
20. Li M, Diehl F, Dressman D, Vogelstein B, Kinzler KW. BEAMing up for detection and quantification of rare sequence variants. *Nat Methods.* 2006; 3:95–97. [PubMed: 16432518]
21. Kinde I, Wu J, Papadopoulos N, Kinzler KW, Vogelstein B. Detection and quantification of rare mutations with massively parallel sequencing. *Proc Natl Acad Sci U S A.* 2011; 108:9530–9535. [PubMed: 21586637]
22. Hoffmann C, Minkah N, Leipzig J, et al. DNA bar coding and pyrosequencing to identify rare HIV drug resistance mutations. *Nucleic Acids Res.* 2007; 35:e91. [PubMed: 17576693]
23. Snyder TM, Khush KK, Valantine HA, Quake SR. Universal noninvasive detection of solid organ transplant rejection. *Proc Natl Acad Sci USA.* 2011; 108:6229–6234. [PubMed: 21444804]
24. Devaney SA, Palomaki GE, Scott JA, Bianchi DW. Noninvasive fetal sex determination using cell-free fetal DNA: a systematic review and meta-analysis. *JAMA.* 2011; 306:627–636. [PubMed: 21828326]



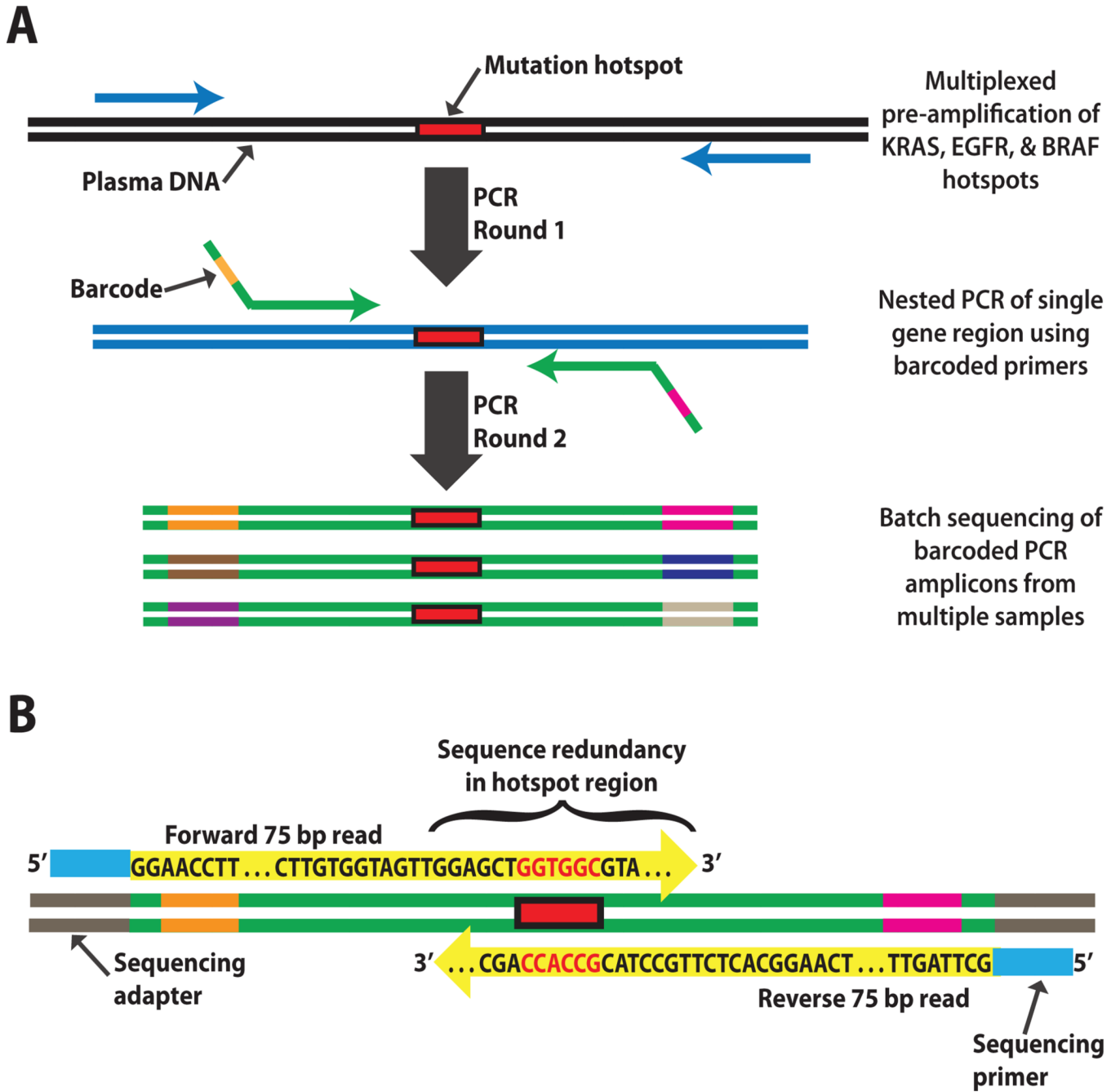


**Fig. 1. Schematic of the error-suppressed multiplexed deep sequencing approach**  
 (A) Cell-free DNA purified from plasma undergoes two rounds of amplification by PCR. The first round amplifies mutation hotspot regions of several genes from a given sample in a single tube. The second round separately amplifies each hotspot region using nested primers incorporating unique combinations of barcodes to label distinct samples. The barcoded PCR products are then pooled and subjected to deep sequencing. Millions of sequences are sorted and counted to determine the ratio of mutant to wild-type molecules derived from each sample. The total number of plasma DNA fragments is measured by real-time PCR and can be used to calculate the absolute concentration of mutant ctDNA. (B) Sequence redundancy in mutation hotspot regions is produced by partial overlap of paired-end reads from the

forward and reverse strands of each clone. This yields highly accurate base-calls, permitting detection and quantitation of rare mutations with greater sensitivity.

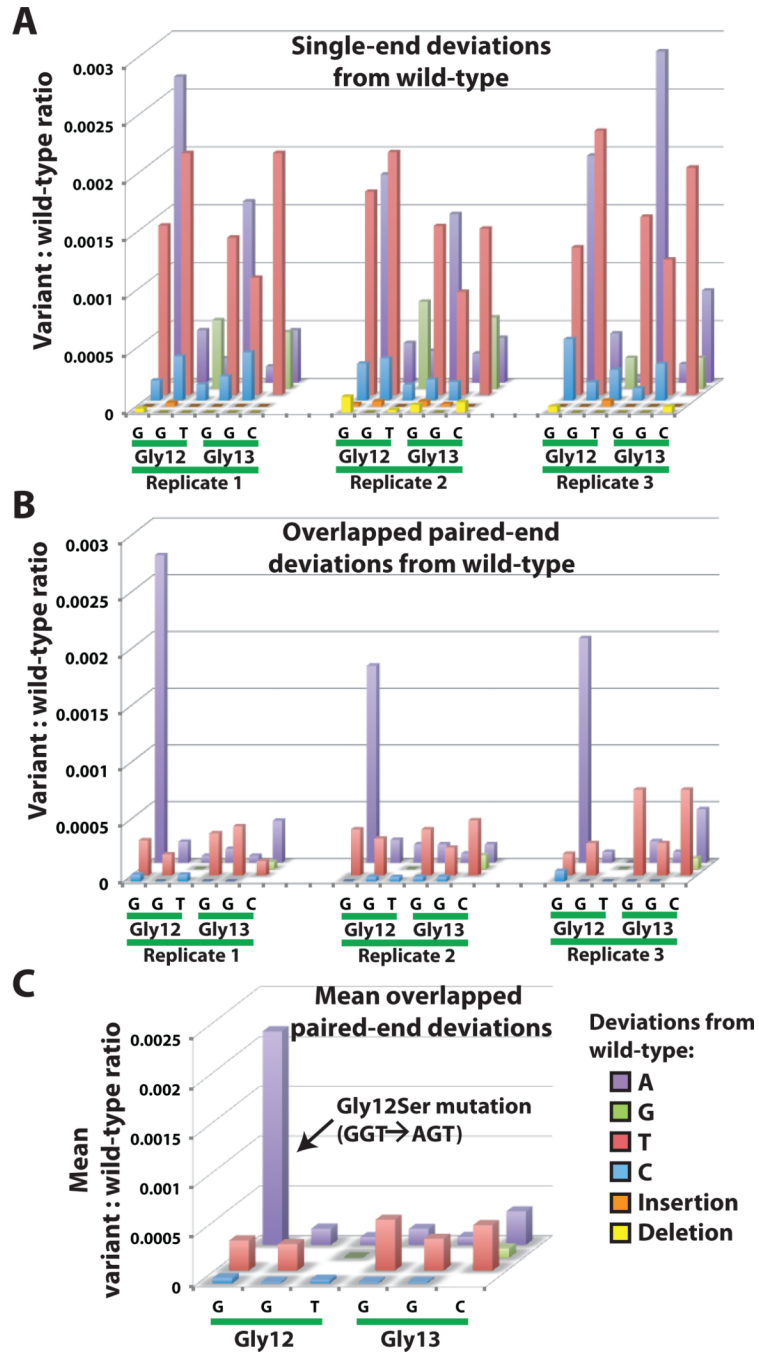


**Fig. 2. Suppression of spurious mutation counts to reveal low-abundance variants**  
 Each bar indicates the frequency of a particular deviation from the wild-type sequence occurring within the codon 12/13 hotspot region of *KRAS*. The tested sample contains 0.2% DNA derived from a lung cancer cell line that is known to be homozygous for a *KRAS* Gly12Ser mutation. **(A)** Filtered reads from one end of the amplicon have relatively frequent mismatches when directly compared to the wild-type sequence. Data from 3 replicate amplifications are shown. **(B)** Sequencer errors are greatly reduced by requiring both partially overlapping paired-end reads from each clone to exactly match a specific mutation. The Gly12Ser mutation is now readily distinguished from the remaining low-level errors

that were likely introduced during DNA amplification and processing. Insertions and deletions are no longer seen in this region after requiring agreement of overlapped reads. (C) A further reduction in the relative error level can be achieved by calculating the mean values of 3 replicate measurements, since mutations found in the original DNA sample should produce more consistent counts than randomly occurring errors.

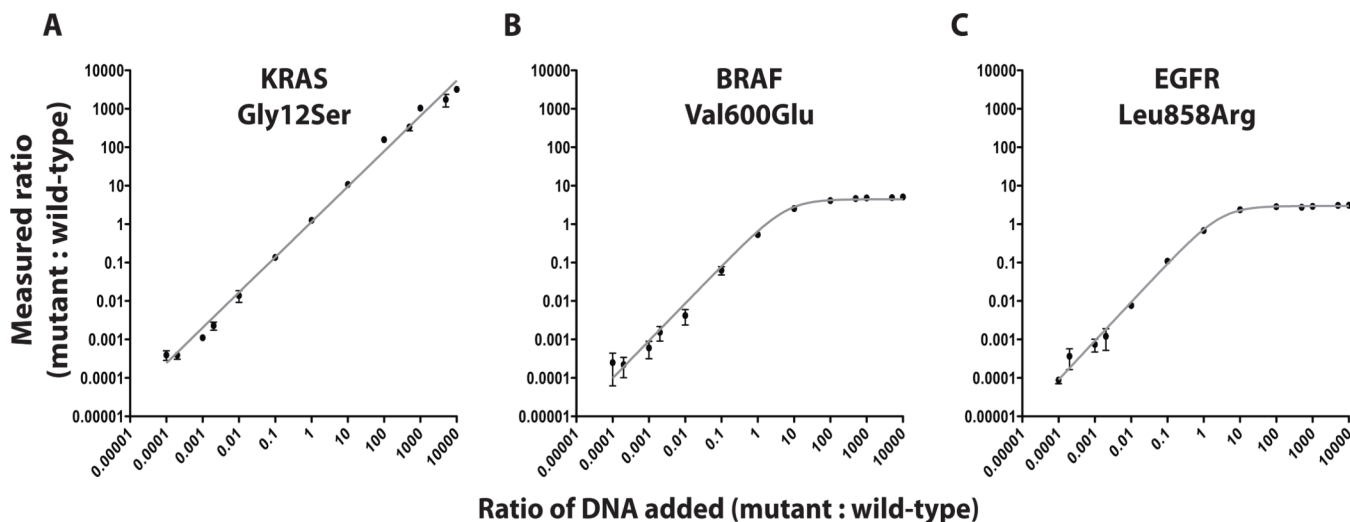


**Fig. 3. Performance of the error-suppressed deep sequencing approach**

Measurements of DNA extracted from mutant and wild-type cancer cell lines mixed in various ratios ranging from 1:10,000 to 10,000:1 show a high degree of accuracy and reproducibility. (A) DNA from the KRAS-mutant cell line produces a linear plot over the range of concentrations tested. (B), (C) BRAF- and EGFR-mutant lines contained a small amount of wild-type DNA, thereby yielding a plateau at higher mutant to wild-type ratios. Non-linear least-squares fits were performed using the equation  $y = 10^{(\text{slope} \cdot \log((1-C) \cdot x / (C \cdot x + 1))) + \text{intercept}}$  where C was the fraction of wild-type molecules found in DNA extracted from mutant cell lines. Error bars indicate the standard deviation of 3 measurements.



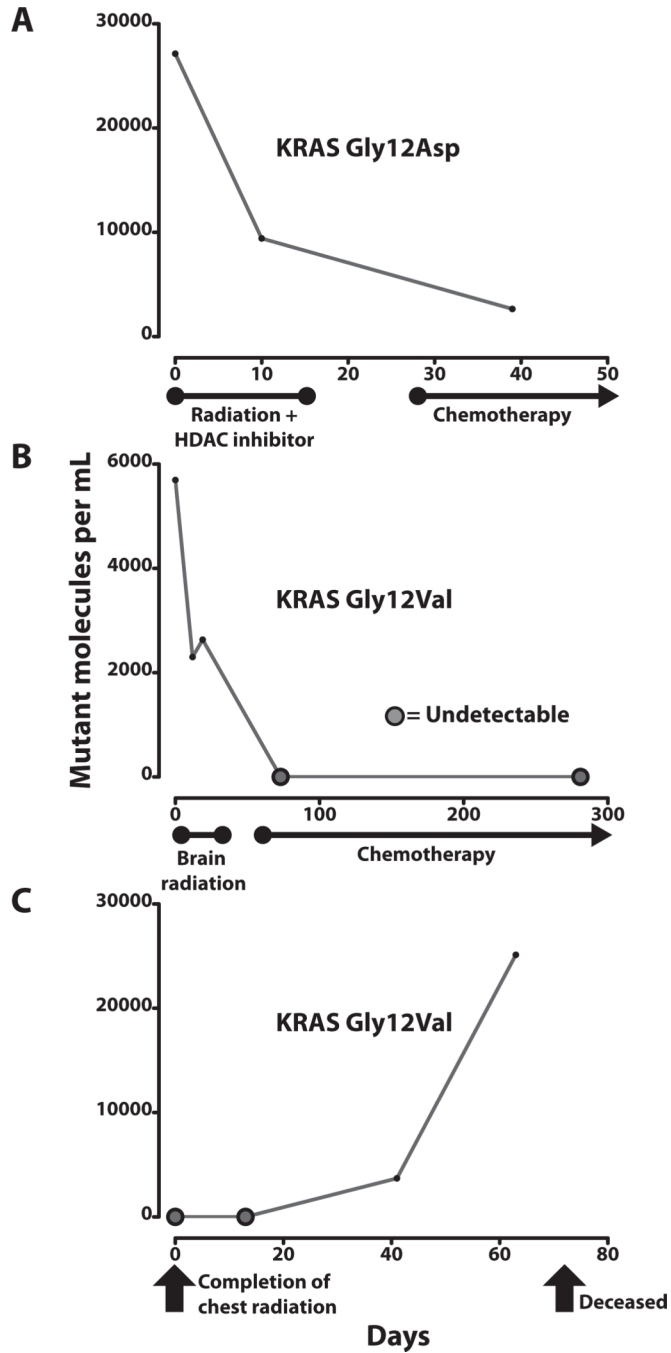


**Fig. 4. Changes in ctDNA levels with treatment or disease progression**

Measurements of mutant ctDNA from patients with NSCLC are shown at various times in relation to therapeutic interventions and disease status. ctDNA was considered undetectable if sequence counts yielded a quantity of less than one mutant molecule per sample. Median genome equivalents per sample, as determined by real-time PCR were 9602 (IQR = 5412–11513) (A) Patient 3 had stage IV lung adenocarcinoma with a 4.3 cm right upper lobe tumor and large metastases in the abdomen and supraclavicular region. She was treated concurrently with an experimental histone deacetylase (HDAC) inhibitor and palliative radiation therapy directed at her painful 6.9 cm supraclavicular lesion. She began

chemotherapy treatment shortly afterwards. **(B)** Patient 5 had a 7.5 cm lung adenocarcinoma with eight small brain metastases ranging from 3 mm to 15 mm in size at presentation. He was treated with palliative whole-brain radiation therapy, followed by long-term weekly chemotherapy. Follow-up imaging revealed an excellent, durable response with shrinkage of the lung tumor to ~15% of its original volume at 7 months after diagnosis. No evidence of disease progression was seen during this time period. **(C)** Patient 9 underwent definitive radiation treatment for locally advanced, stage IIIB undifferentiated NSCLC. Other health conditions prevented him from undergoing surgery or concurrent chemotherapy. Blood sample collection commenced upon completion of his treatment. Although his disease was confined to the thorax prior to initiating radiation therapy, a PET scan performed 8 weeks after treatment showed marked progression of disease with multiple osseous, hepatic, and subcutaneous metastases. He expired 10 weeks after completing treatment.